Available online at www.sciencedirect.com
ScienceDirect
Journal of Hazardous Materials 156 (2008) 201–207
Journal of Hazardous Materials
www.elsevier.com/locate/jhazmat

Molecular dynamics study of the structure and performance of simple and double bases propellants

Xiufang Ma, Weihua Zhu, Jijun Xiao, Heming Xiao *

Institute for Computation in Molecular and Material Science, Nanjing University of Science and Technology, Nanjing 210094, PR China

Received 7 November 2006; received in revised form 6 December 2007; accepted 6 December 2007
Available online 20 February 2008

Abstract

To investigate the structure and performance of simple and double bases propellants, the nitrocellulose (NC), nitroglycerin (NG), and double mixed system (NC + NG) have been simulated by using the molecular dynamics (MD) method with the COMPASS force field. The interactions between NC and NG have been analyzed by means of pair correlation functions. The mechanical properties of the three model systems, i.e. elastic coefficients, modulus, Cauchy pressure, and Poisson's ratio, etc., have been obtained. It is found that the rigidity, ductibility, and tenacity of the double bases propellants (NC + NG) are stronger than those of simple base propellants (NC), which attributes to the effect of NG and the strong interactions between NC and NG. The detonation properties of the three systems have also been calculated and the results show that compared with the simple base propellant (NC), the detonation heat and detonation velocity of the double base propellants (NC + NG) are increased.

Keywords: Molecular dynamics (MD); Propellant; Mechanical property; Detonation property

1. Introduction

Propellant, known as a kind of energetic materials for launching, usually contains fuel and oxidizer components. It has widespread application in weapon equipment, space navigation, and industrial and agricultural production, so researches on propellant have received great attention for a long time. A typical simple base propellant consists of a simple compound, usually nitrocellulose (NC), and a double bases propellant usually consists of NC and nitroglycerin (NG), to which a plasticizer is added [1–4]. Both simple base and double bases propellants are homogeneous. Modern composite propellants are heterogeneous mixtures, which use a crystallized salt as an oxidizer and aluminum as fuel. For a composite propellant, the relationship between its formulation and performance plays a key role in its formulation design. Therefore, much experimental work has been done to investigate the issues related to the structure, formulation, and properties of propellants. Computer simulations have increasingly played an important role in this field. They can make it possible to screen candidate formulation designs, thereby avoiding expensive experimental tests. In addition, simulations may provide an understanding of the structure–performance relationships in propellants, which in turn can help design better and more efficient laboratory tests.

A force field method, especially molecular dynamics (MD) method, is an important and effective method to study the structure and performance of materials at present. Recently, our institute firstly utilizes MD method to study the polymer-bonded explosive (PBX), a composite material [5–12]. Yet there is no MD-based studies reported on this kind of propellant. In this study we choose simple and double bases propellants as an example to investigate the structure–performance relationships. The destination in this study is to test the force field, method, and model, and to understand the correlations between the structure and performance for propellants. It is hoped that our studies provide some information and guidance for composite formulation design.

2. Computational approach and details

2.1. Computational model

The initial models were built by using materials studio (MS) package [13]. As for NC, the backbone conformation is critical to

* Corresponding author. Tel.: +86 25 84303919; fax: +86 25 84303919.
E-mail address: xiao@mail.njust.edu.cn (H. Xiao).

0304-3894/$ – see front matter © 2007 Elsevier B.V. All rights reserved.
doi:10.1016/j.jhazmat.2007.12.068

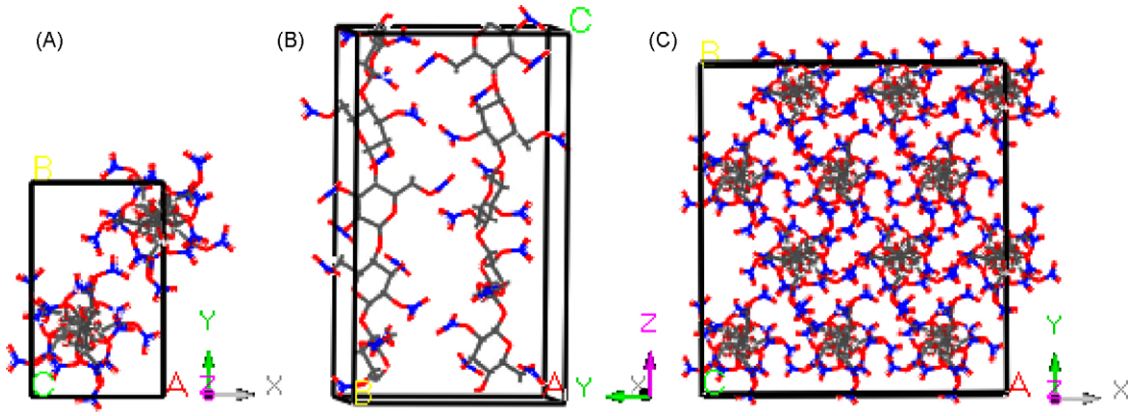

Fig. 1. The primitive cell of NC and its supercell (3 × 2 × 1) (C). (A) Top view, (B) side view and (C) initial model of simple base propellant.

its performance. Due to lacking of the whole bulk cell parameters and space group of NC, we built its molecular chain with 5_2 helix conformation suggested by Meader et al. [14]. Two chains of polymer NC were placed in a periodic box with the lattice vectors of $a = 0.90$ nm, $b = 1.46$ nm, and $c = 2.54$ nm, the lattice angles of $\alpha = \beta = \gamma = 90°$, and the density of 1.49 g cm^{-3}. Therefore, the primitive cell of NC was obtained (see Fig. 1A and B) and the initial model of simple base propellant was established and shown in Fig. 1C.

The initial β-nitroglycerin (NG) structure was built based on X-ray diffraction data [15], with four molecules in a cell and Fig. 2 shows its primitive cell and supercell. When the hydroxyl groups (–OH) of cellulose are replaced by nitro groups (–NO_2), the products are obtained with one, two or three substitutions and their nitrogen containing (N%) is 6.75, 11.11, and 14.14%, respectively. In fact, we always get their mixture with diverse substitution products due to difficulty in being nitrified completely. The simple base propellant with nitrogen containing of 13.0% or above, was built from cellulose trinitrate in order to simplify the model.

As for the double bases propellant with its nitrogen containing of 12.0%, we built the initial model as follows in order to meet the practical requirement of composite design. To emphasize the interaction between NC and NG, we choose the side of NC, not the end groups, to contact NG because of the nitro groups existing in outer side of the helix chain of NC. The double bases propellant model contains 10 helix NC chains and 43 NG molecules, with mass percentage of 58.1 and 41.9%, respectively, and is shown in Fig. 3.

Therefore, we get the three initial models for the MD simulations, as shown in Figs. 1C, 2B and 3.

2.2. MD simulations

The COMPASS force field [16] is used to study the structures and properties of the NC, NG, and NC + NG. Its parameters have been debugged and ascertained from the *ab initio* calculations, optimized according to the experimental values, and parameterized using extensive data for molecules in condensed phase. Its nonbonded parameters have been further amended and val-

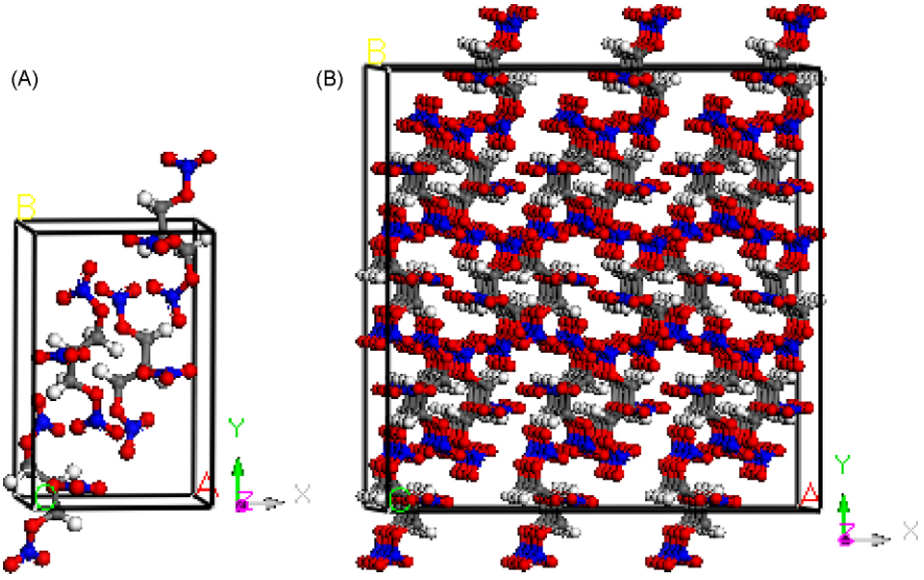

Fig. 2. The primitive cell and supercell of β-nitroglycerin (NG). (A) Primitive cell and (B) supercell (3 × 2 × 4) of NG.

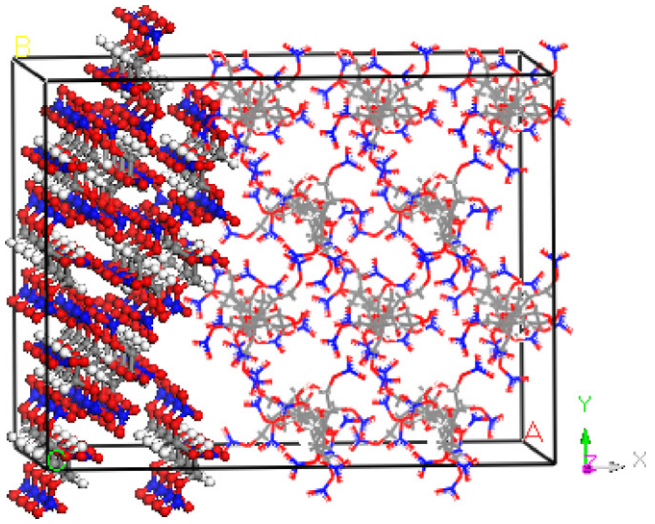

Fig. 3. The initial model of double bases propellant. The left is NG and the right is NC.

idated by the thermal physical properties of the molecules in liquid and solid phases obtained using the MD method. Consequently, COMPASS is able to accurately predict the structural, conformational, vibrational, and thermophysical properties for a broad range of compounds in both isolation and condensed phases. Extensive validations have been performed [16–18]. The results are in good agreement with those from experiments. On the other hand, this force field has been successfully employed to investigate the nitrate esters [16]. It is therefore suitable for performing MD simulations on them.

The present molecular dynamics simulations of NC, NG, and NC + NG were performed using the COMPASS force field and periodic boundary conditions. The MD simulations were conducted at constant volume and constant temperature (NVT) conditions. After an equilibrium run, the module allows one to collect the results of the dynamics simulation in a trajectory file. Through analyzing trajectory files, the static elastic properties and pair correlation functions were obtained. Considering the condition of equilibrium and spend of CPU time, all the simulation time is added to 0.2–0.3 ns. In the above-mentioned MD simulations, temperature controls were treated using Andersen method [19]. Nonbonded interactions, spline width, and buffer width were truncated at 0.95, 0.1 and 0.05 nm, respectively. All the calculations were implemented on a Pentium IV PC.

2.3. Calculations of mechanical properties

Mechanical properties are estimated by using the loading experiments of MD simulation in MS. The loading experiment is the simplest but the most important and extensive method to measure the mechanical properties, such as elastic and plastic property, strain hardening and ductility, and so on [20]. By means of small deform loading experiment, the elastic tensile stress can be accomplished. A total of three loading experiments is performed, in which a uniaxial tensile stress is applied stepwise along the x, y or z directions. For each

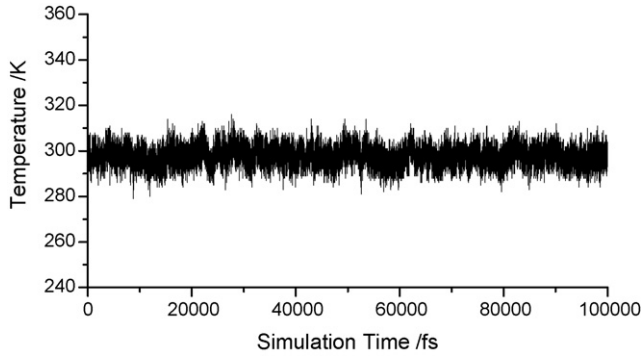

Fig. 4. Plot of temperature vs. simulation time for NC + NG.

loading direction, constant stress dynamics is performed in a series of up to 10 stages, each of duration 1 ps. At the end of each stage, the values of the internal stress tensor and the strain tensor are recorded. So the Hooke's law is easy to get, which explicitly describes the stress–strain behavior of a material. When more than one frame is analyzed, stress–strain data are averaged for all the frames. The Young's modulus (tensile modulus, E) and Poisson's ratio (υ) are computed from the least-squares fits of the averaged tensile stress versus tensile strain, and of the (negative) average lateral strain versus tensile strain [21].

The Young's modulus (E) and Poisson's ratio (υ) may be written in terms of the Lamé coefficients (μ and λ) as follows: $E = \mu(3\lambda + 2\mu)/(\lambda + \mu)$, $\upsilon = \lambda/2(\lambda + \mu)$. From this two formulas, one can calculate μ and λ, while bulk modulus (K) and shear modulus (G) can be extracted through $K = \lambda + 2\mu/3$ and $G = \mu$.

3. Results and discussion

3.1. Criteria of system equilibrium

There are two criteria to judge the equilibrium: one is the equilibrium of temperature and the other is the equilibrium of energy. The fluctuations of temperature and energy are in the range of 5–10%, that is to say, the fluctuation of temperature is within ±15 K and the energy is invariable or small fluctuation around the average energy value. The MD systems here have reached the equilibrium, as shown in Figs. 4 and 5.

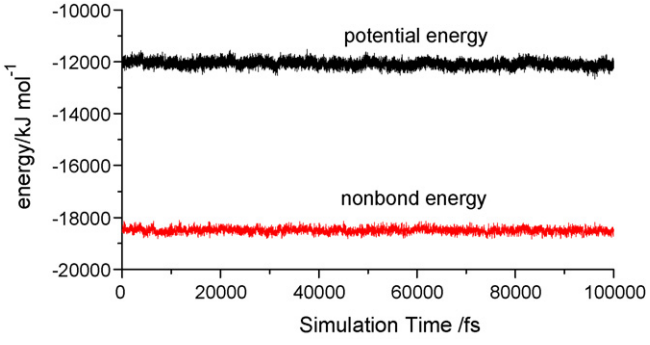

Fig. 5. Plot of energy vs. simulation time for NC + NG.

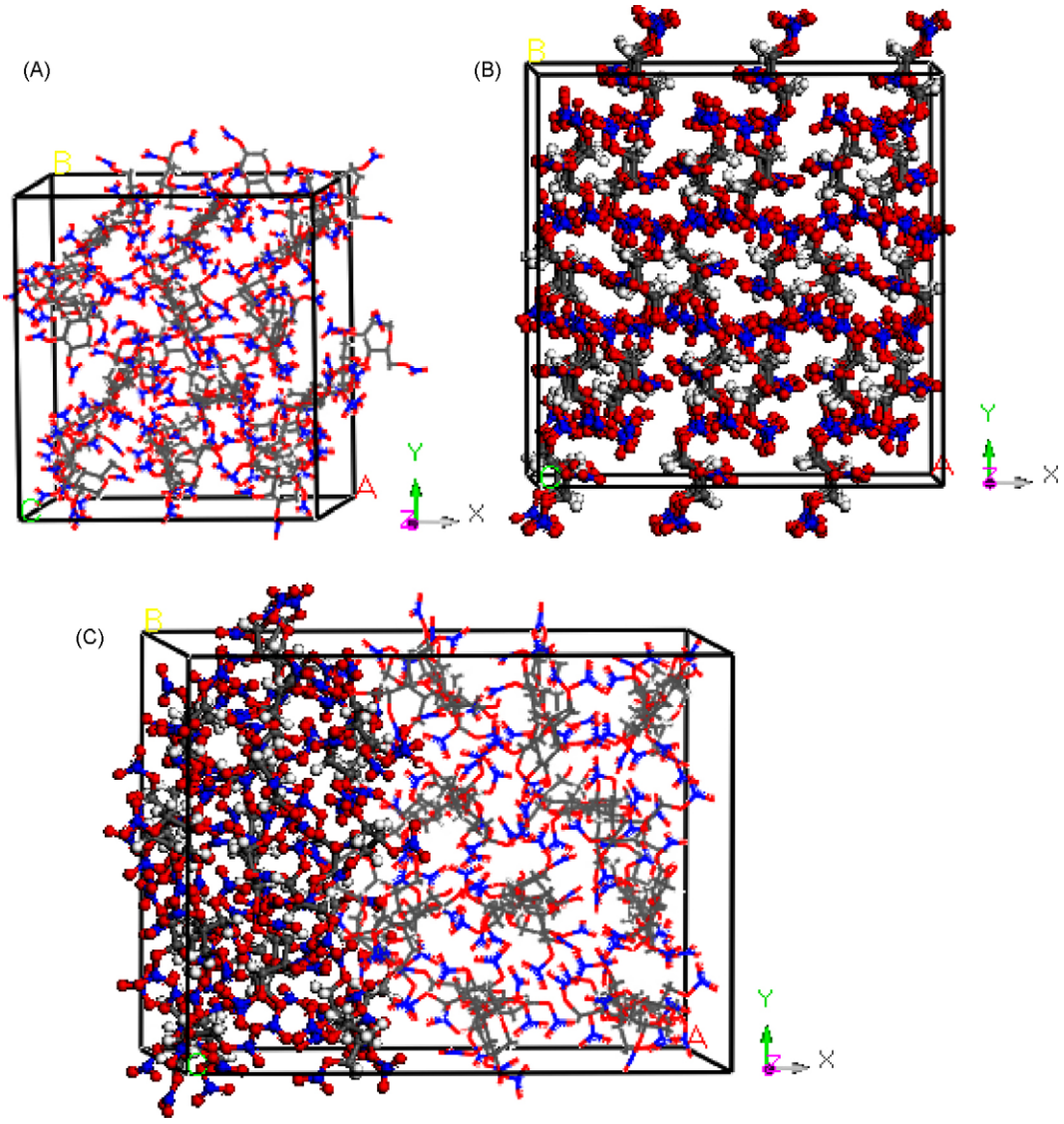

Fig. 6. The equilibrium configurations after MD. (A), (B) and (C) are the equilibrium configurations of NC, NG, and NC + NG, respectively.

3.2. Equilibrium configuration and interactions between constituents

After the MD simulations, one can get the equilibrium configurations of the three models. Fig. 6 illustrates the equilibrium configurations of NC (A), NG (B), and double constituents system (NC + NG) (C), respectively.

Comparing the equilibrium configuration of NC with that before MD (Fig. 1C), part of the helix backbone of NC after MD is slightly uncoiled due to the rotation and torsion of flexible chain. The configuration of NG is hardly changed after MD, while the interface of double constituents system NC + NG is changed much owing to the interactions between NC and NG.

From the equilibrium configuration of trajectory files after MD, the energy of the system NC + NG (E_{total}) reaches $-12{,}189.8\,kJ\,mol^{-1}$. The energy of NC ($E_{NC}$) is $-1542.3\,kJ\,mol^{-1}$ by moving NG from the equilibrium system NC + NG. When NC is removed from the system, the energy of NG (E_{NG}) can be got. So the binding energy between NC and NG can be calculated according to $\Delta E = -(E_{total} - E_{NC} - E_{NG})$, which is shown in Table 1. It can be seen that there exist the interactions between NC and NG.

The interactions between each constituent can be further analyzed by examining pair correlation function. The pair correlation function gives a measure of the probability of finding another atom at a distance r from a specific atom. It has many applications in structural investigations of both solid and liquid packing (local structure), in studying specific interactions such as hydrogen bonding, and in statistical mechanical theories of liquids and mixtures.

Table 1
Binding energy between NC and NG in double constituents system ($kJ\,mol^{-1}$, 298 K)

E_{total}	−12189.8
E_{NC}	−1542.3
E_{NG}	−8281.5
ΔE	2366.0

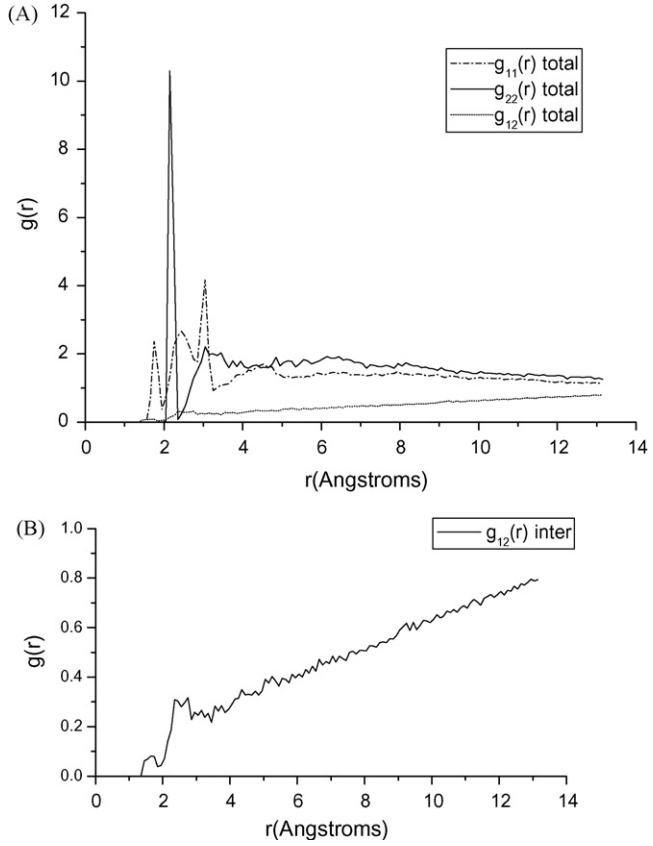

Fig. 7. The pair correlation functions for H(NC) and O(NG) (A and B).

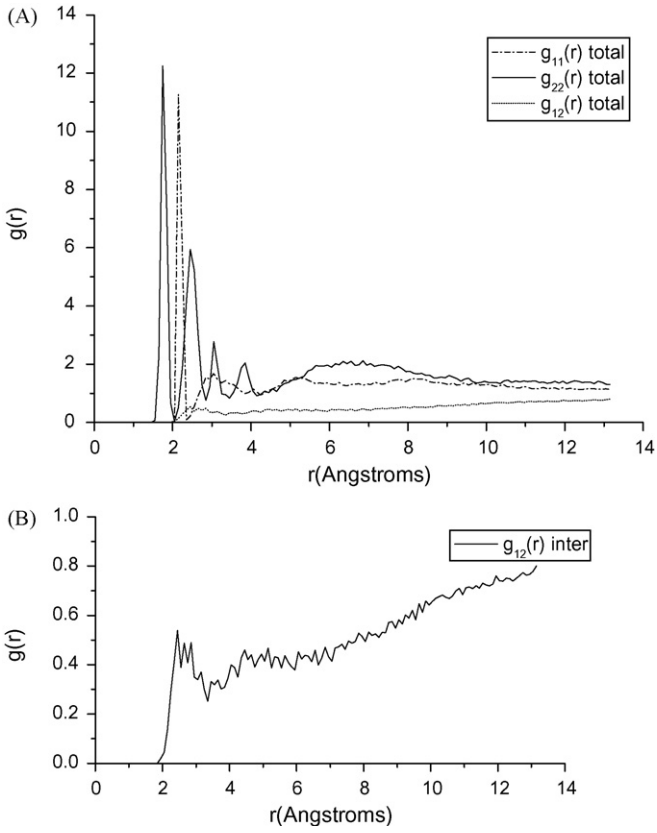

Fig. 8. The pair correlation functions for O(NC) and H(NG) (A and B).

In general, intermolecular actions include hydrogen bonding action and van der Waals (vdw) force, in which the vdw force is composed of dipole–dipole, induction, and dispersion force. If the distance between atoms is 2.6–3.1, 3.1–5.0 or above 5.0 Å, the interaction belongs to hydrogen bonding, strong vdw, or weak vdw force, respectively. Although the hydrogen bonding action is weaker than chemical bond, it is the strongest force among intermolecular actions and can strengthen them.

As for NC and NG, the hydrogen bonding may exist between H(O) of NC and O(H) of NG, so the pair correlation functions should be analyzed separately. When the pair correlation functions of H(NC) and O(NG) are analyzed, H(NC) and O(NG) are sets 1 and 2, respectively. Then the pair correlation function analysis can be performed on two sets and the results are shown in Fig. 7. When these of O(NC) and H(NG) are analyzed, the former is set 1 and the latter set 2. The results are shown in Fig. 8.

Fig. 7 shows the pair correlation function results of H(NC) and O(NG). Fig. 7A presents three total results of set 1, set 2, and two sets, i.e. $g_{11}(r)$ total, $g_{22}(r)$ total, and $g_{12}(r)$ total. Each result includes inter- and intra-molecular interactions, that is, $g_{11}(r)$ total = $g_{11}(r)$ inter + $g_{11}(r)$ intra, $g_{22}(r)$ total = $g_{22}(r)$ inter + $g_{22}(r)$ intra, $g_{12}(r)$ total = $g_{12}(r)$ inter + $g_{12}(r)$ intra. But the $g_{12}(r)$ inter is closely related to the interactions of double constituents. So we draw $g_{12}(r)$ inter from the total results and made further analysis on it. The result of $g_{12}(r)$ inter is shown in Fig. 7B.

From Fig. 7B, we can see the probability distribution for H(NC) and O(NG) atoms. Within the scope of 0–5.0 Å, a peak locates in 2.3–2.8 Å, which suggests that there is a high probability for the two atoms in the distance and the interaction between them belongs to hydrogen bonding action. Part of the peaks lies in 4.0–5.0 Å and the interaction belongs to strong vdw force. So, there are the hydrogen bonding action and strong vdw force between H(NC) and O(NG).

Similarly, Fig. 8 illustrates the pair correlation function results for O(NC) and H(NG). Within the scope of 0–5.0 Å in Fig. 8B, the peaks locate in 2.0–3.0 Å or 4.0–5.0 Å, the interaction between them belongs to hydrogen bonding and strong vdw force, separately.

Therefore, there is the hydrogen bonding action and strong vdw force between NC and NG, which is the main cause of the strong interactions between them. Moreover, most of the hydrogen bonding actions exist between O(NC) and H(NG).

3.3. Mechanical property

It is known from elastic mechanics that the generalized Hooke's law can be written as follows [19]

$$\begin{bmatrix} \sigma_x \\ \sigma_y \\ \sigma_z \\ \tau_{yz} \\ \tau_{zx} \\ \tau_{xy} \end{bmatrix} = \begin{bmatrix} C_{11} & C_{12} & C_{13} & C_{14} & C_{15} & C_{16} \\ C_{21} & C_{22} & C_{23} & C_{24} & C_{25} & C_{26} \\ C_{31} & C_{32} & C_{33} & C_{34} & C_{35} & C_{36} \\ C_{41} & C_{42} & C_{43} & C_{44} & C_{45} & C_{46} \\ C_{51} & C_{52} & C_{53} & C_{54} & C_{55} & C_{56} \\ C_{61} & C_{62} & C_{63} & C_{64} & C_{65} & C_{66} \end{bmatrix} \begin{bmatrix} \varepsilon_x \\ \varepsilon_y \\ \varepsilon_z \\ \gamma_{yz} \\ \gamma_{zx} \\ \gamma_{xy} \end{bmatrix}$$

Table 2
Mechanical properties of NC, NG and (NC + NG) (GPa, 298 K)

	NC	NG	NC + NG
C_{11}	3.4	12.7	7.2
C_{22}	4.6	26.4	7.0
C_{33}	5.5	13.1	10.3
C_{44}	1.2	4.1	1.7
C_{55}	1.3	5.9	1.8
C_{66}	1.4	4.8	1.7
C_{12}	1.1	3.4	3.4
C_{13}	0.6	7.7	2.5
C_{23}	0.7	0.8	2.6
C_{15}	−0.2	0.0	−0.2
C_{25}	−0.1	0.0	0.2
C_{35}	0.3	0.0	−0.3
C_{46}	0.0	0.0	0.0
Tensile modulus (E)	4.2	16.0	6.7
Poisson's ratio (υ)	0.15	0.19	0.26
Bulk modulus (K)	2.0	8.5	4.6
Shear modulus (G)	1.8	6.7	2.7
K/G	1.11	1.27	1.70
C_{12}–C_{44}	−0.1	−0.7	1.7
Density, ρ (g cm^{-3})	1.49	1.84	1.60

Because of the existence of the strain energy, the elastic coefficient matrix of a material should satisfy the formula: $C_{ij} = C_{ji}$, even for an extremely anisotropic body and there are 21 independent elastic coefficients. For an isotropic solid, there are only two independent elastic coefficients (C_{11} and C_{12}). Accordingly, each modulus and Poisson's ratio can be obtained based on two Lamé coefficients ($C_{11} - C_{12} = 2\mu$ and $C_{12} = \lambda$). The program can assume a material as isotropic and calculate the effective isotropic mechanical properties.

The static mechanical properties including elastic coefficients, elastic modulus, Cauchy pressure, and Poisson's ratio of NC, NG, and (NC + NG) are shown in Table 2. Elastic coefficients C_{ij} (i, j = 1–6) manifest that there are different elastic effects everywhere in materials. Elastic modulus, a measurement of rigidity, is the ratio of stress to strain. The larger the tensile modulus of a material is, the stronger its rigidity is [19]. The increase of Poisson's ratio suggests that the plastic property increases. Cauchy pressure (C_{12}–C_{44}), shown in Table 2, can be used as a criterion to evaluate the ductibility and brittleness of a material. Usually, the value of (C_{12}–C_{44}) for a ductile material is positive, contrarily, that is negative for a brittle material. In addition, the ratio (bulk modulus/shear modulus, K/G) can be used to evaluate the tenacity of a material. Usually, the greater the value of K/G is, the better tenacity a material possesses [22].

According to this, in Table 2, the elastic coefficients and modulus of NC are much smaller than those of NG, which suggests the elasticity of NC is stronger than that of NG due to the conformation switch of polymer NC. The tensile modulus of pure NG is 16.0 GPa, which predicts that NG has the strong rigidity to resist deformation, but when an amount of NC is put on it, the tensile modulus decreases to 6.7 GPa, which shows that the elasticity of the obtained double constituents system greatly strengthens. That is, the NC + NG possesses stronger rigidity compared with NC. The Cauchy pressure (C_{12}–C_{44}) of pure NC is −0.1 GPa, and the (C_{12}–C_{44}) of NC + NG is 1.7 GPa, which suggests the ductibility of NC + NG are greatly improved. As for K/G, the value of NC (1.11) is smaller than that of NC + NG (1.70), which manifests the latter has better tenacity than the former. This predicts that the impact tenacity of the double bases propellant has been improved. Thus, the double bases propellant is easy to meet explosive loading.

From Table 2, it can be seen that the tensile modulus of NC is 4.2 GPa, but that of NC + NG is 6.7 GPa, which attributes to the rigid NG. The data in Table 2 predict that pure NC and NG are brittle due to their negative Cauchy pressure, and the Cauchy pressure of NC + NG increases to 1.7 GPa and the ductibility of NC + NG is stronger than that of NC and NG. So, the strengthened ductibility results from the interactions between NC and NG. Similar analysis on K/G illustrates that the strong interaction is the main cause of strengthened tenacity. Therefore, the strong interactions between NC and NG make interface molecule conformation change and do ductibility and tenacity strengthen.

3.4. Detonation heat, detonation velocity, and detonation pressure

Detonation heat, detonation velocity, and detonation pressure are important parameters of an explosive. For pure NC and NG, the detonation velocity and pressure can be obtained according to Kamlet formulas [23], in which the other parameters are from literatures (for instance, Ref. [24]). For the double bases explosive, NC + NG, detonation heat can be obtained based on $Q_v = Q_{v1}m_1 + Q_{v2}m_2 + Q_{v3}m_3$ (m_i is the percentage of mass) and detonation velocity can be got according to ω–Γ formulas [25], $V_D = 33.05Q^{1/2} + 243.2\omega\rho$, where Q, ω, and ρ denotes the characteristic heat, heat factor, and density of explosive, respectively. ρ can be obtained from MD equilibrium configuration. So, the detonation properties of NC, NG, and NC + NG are gotten and listed in Table 3.

From Table 3, it can be seen that the detonation heat, detonation velocity, and pressure of NC are smaller than those of NG but the detonation heat and velocity of NC + NG is larger than those of NC due to the effect of NG.

Therefore, double bases propellant possesses large detonation heat and velocity with improved mechanical properties, strengthened ductibility, and tenacity, which predicts that it has the better comprehensive performance than simple base one.

Table 3
Detonation properties of NC, NG and (NC + NG)

	NC	NG	NC + NG
Density, ρ (g cm^{-3})	1.49	1.84	1.60
Heat of formation, ΔH_f (kcal mol^{-1})	−762.9	−82.4	–
Detonation heat, Q_v (kJ kg^{-1})	4427	6318	5128
Detonation velocity, V_D (m s^{-1})	7297	7700	7573
Detonation pressure, P_D (GPa)	20.9	25.3	–

4. Conclusions

By the MD simulations and theoretical calculations of the title substances, several conclusions can be drawn:

(1) The COMPASS force field is fit for the simulations of NC, NG, and NG + NG systems.
(2) Compared with simple base propellant (NC), the elasticity of double bases one (NC + NG) decreases and its rigidity increases, which attributes to the effect of NG; moreover, its ductibility and tenacity increase, which attributes to the strong interactions between NC and NG.
(3) The detonation heat and velocity of double bases propellant is larger than those of simple base one due to the effect of NG.
(4) Complex effects in the constituents should be taken into account in the design of composite propellants. MD simulation may provide some theoretical information and guidance for composite propellant design.

Acknowledgment

This work was supported by national "973" project.

References

[1] S. Bernard, S. Leroy, Energeties of Propellant Chemistry, Wiley, New York, 1964.
[2] R.F. Gould, Propellants Manufacture, Hazards and Testings, ACS Advances in Chemistry Series 88, Washington, 1969.
[3] Z.S. Wang, Y.X. Ou, W.Z. Ren, Science and Technology of Explosives, Beijing Institute of Technology Press, Beijing, 2002.
[4] L.F. Hou, Composite Solid Propellants, Astronavigation Press, Beijing, 1994.
[5] J.J. Xiao, G.Y. Fang, G.F. Ji, H.M. Xiao, Simulation investigation in the binding energy and mechanical properties of HMX-based polymer-bonded explosives, Chin. Sci. Bull. 50 (2005) 21–26.
[6] X.F. Ma, J.J. Xiao, H. Huang, W. Zhu, J.S. Li, H.M. Xiao, Effects of concentration and temperature on mechanical properties of TATB/PCTFE PBX by molecular dynamics simulation, Acta Chim. Sin. 63 (2005) 2037–2041.
[7] J.J. Xiao, Y.C. Huang, Y.J. Hu, H.M. Xiao, Molecular dynamics simulation of mechanical properties of TATB/flourine-polymer PBXs along different surfaces, Sci. Chin. B 48 (2005) 504–510.
[8] J.J. Xiao, X.F. Ma, W. Zhu, Y.C. Huang, H.M. Xiao, Molecular dynamics simulations of polymer-bonded explosives (PBXs): modeling, mechanical properties and their dependence on temperatures and concentrations of binders, Propell. Explos. Pyrotech. 32 (2007) 355–359.
[9] X.F. Ma, J.J. Xiao, H. Huang, X.H. Ju, J.S. Li, H.M. Xiao, Simulative calculation on mechanical property, binding energy and detonation property of TATB/fluorine-polymer PBX, Chin. J. Chem. 24 (2006) 473–477.
[10] X.J. Xu, J.J. Xiao, W. Zhu, H.M. Xiao, H. Huang, J.S. Li, Molecular dynamics simulations for pure ε-CL-20 and ε-CL-20-based PBXs, J. Phys. Chem. B 110 (2006) 7203–7207.
[11] X.F. Ma, F. Zhao, J.J. Xiao, G.F. Ji, W. Zhu, H.M. Xiao, Simulation study of structure and performance of HMX based PBX, Explos. Shock Wave 27 (2007) 109–115.
[12] L. Qiu, H.M. Xiao, W.H. Zhu, J.J. Xiao, W. Zhu, Ab initio and molecular dynamics study of crystalline TNAD (*trans*-1,4,5,8-tetranitro-1,4,5,8-tetraazadecalin), J. Phys. Chem. B 110 (2006) 10651–10661.
[13] Material Studio 3.0, discover/Accelrys: San Diego, CA, 2004.
[14] D. Meader, E.D.T. Atkins, F. Happey, Cellulose trinitrate: molecular conformation and packing considerations, Polymer 19 (1978) 1371–1374.
[15] A.A. Espenbetov, M.Y. Antipin, Y.T. Struchkov, et al., Structure of 1,2,3-propanetriol trinitrate (β-modification), $C_3H_5N_3O_9$, Acta Crystallogr. C 40 (1984) 2096–2098.
[16] S.W. Bunte, H. Sun, Molecular modeling of energetic materials: the parameterization and validation of nitrate esters in the COMPASS force field, J. Phys. Chem. B 104 (2000) 2477–2489.
[17] H. Sun, D. Rigby, Polysiloxanes: ab initio force field and structural, conformational, and thermophysical properties, Spectrochim. Acta A 53 (1997) 1301–1323.
[18] H. Sun, An ab initio force-field optimized for condense-phase applications—overview with details on alkanes and benzene compounds, J. Phys. Chem. B 102 (1998) 7338–7364.
[19] H.C. Andersen, Molecular dynamics simulations at constant pressure and/or temperature, J. Chem. Phys. 72 (1980) 2384–2393.
[20] X.L. Zhen, Mechanical Properties of Engineering Materials, Northwestern Polytechnical University Press, Xi'an, 2004.
[21] J.L. Wu, Elastic Mechanics, Tongji University Press, Shanghai, 1993.
[22] S.F. Pugh, Relations between the elastic moduli and the plastic properties of polycrystalline pure metals, Phil. Mag. A 45 (1954) 823–843.
[23] M.J. Kamlet, S.J. Jacobs, Chemistry of detonations. I. A simple method for calculating detonation properties of C–H–N–O explosives, J. Chem. Phys. 48 (1968) 23–35.
[24] X.F. Zhang, Handbook on Performance of Explosive Materials in Foreign, Enginery Industry Publishing House, Beijing, 1991.
[25] X. Wu, Simple method for calculating detonation parameters of explosive, Energ. Mater. 3 (1985) 263–277.